AWARD NUMBER: W81XWH-14-1-0049

TITLE: Using T2-Exchange from Ln3+DOTA-Based Chelates for Contrast-Enhanced Molecular Imaging of Prostate Cancer with MRI

PRINCIPAL INVESTIGATOR: Todd C. Soesbe, Ph.D.

CONTRACTING ORGANIZATION: University of Texas Southwester Medical Center at Dallas
Dallas, Texas 75390-8568

REPORT DATE: April 2015

TYPE OF REPORT: Annual

PREPARED FOR: U.S. Army Medical Research and Materiel Command
Fort Detrick, Maryland 21702-5012

REPORT DOCUMENTATION PAGE

Form Approved
OMB No. 0704-0188

1. REPORT DATE	2. REPORT TYPE	3. DATES COVERED
April 2015	Annual	1 Feb 2014 - 31 Jan 2015

4. TITLE AND SUBTITLE

Using T2-Exchange from Ln3+DOTA-Based Chelates for Contrast-Enhanced Molecular Imaging of Prostate Cancer with MRI

5a. CONTRACT NUMBER

5b. GRANT NUMBER
W81XWH-14-1-0049

5c. PROGRAM ELEMENT NUMBER

6. AUTHOR(S)
Todd C. Soesbe, Ph.D.
Yunkou Wu, Ph.D.
James Ratnaker, Ph.D.
Mark Milne, Ph.D.
Lei Zhang
A. Dean Sherry, Ph.D.

E-Mail: todd.soesbe@utsouthwestern.edu

5d. PROJECT NUMBER

5e. TASK NUMBER

5f. WORK UNIT NUMBER

7. PERFORMING ORGANIZATION NAME(S) AND ADDRESS(ES)

UT Southwestern Medical Center at Dallas
5323 Harry Hines BLVD, Dallas, Texas, 75390-8568

8. PERFORMING ORGANIZATION REPORT NUMBER

9. SPONSORING / MONITORING AGENCY NAME(S) AND ADDRESS(ES)

U.S. Army Medical Research and Materiel Command
Fort Detrick, Maryland 21702-5012

10. SPONSOR/MONITOR'S ACRONYM(S)

11. SPONSOR/MONITOR'S REPORT NUMBER(S)

12. DISTRIBUTION / AVAILABILITY STATEMENT

Approved for Public Release; Distribution Unlimited

13. SUPPLEMENTARY NOTES

14. ABSTRACT

Purpose: To develop a targeted T_2-exchange MRI contrast agent for the early detection and diagnosis of prostate cancer.

Scope: This contrast agent is based on T_2 contrast (i.e., hypo-intense contrast) arising from water molecule exchange between the inner-sphere of a Dysprosium (Dy3+) central ion and the bulk water. The level of this "T_2-exchange" contrast is highly dependent on both the water molecule exchange rate and the paramagnetic shift of the water molecule hydrogen protons when bound to the Dy3+ ion. After identifying which DyDOTA-based chelate gave the optimal water molecule exchange rate at 9.4 T MRI, the chelate would then be polymerized to increase the transverse relaxivity (r_2) per molecule by 100 fold. Thereby creating a highly sensitive, low molecular weight T_2 contrast agent for cancer molecular imaging with MRI. Polymers targeting the prostate specific membrane antigen (PSMA) of prostate cancer cells would then be synthesized and tested with both *in vitro* and *in vivo* experiments.

Major Findings: We found that the DyDOTA-$(gly)_2$ and DyDOTA-$(gly)_3$ chelates had almost ideal water molecule exchange rates at 9.4 T and 37 degrees Celsius, which gave them transverse relaxivities (r_2) that were close to the theoretical maximum predicted by Swift-Connick theory. These two chelates were then chosen as candidates for polymerization. We also found that the paramagnetic shift in the bound water molecule hydrogen protons for each DyDOTA-based chelate was dependent on temperature. Details of these experiments and results are given in our Magnetic Resonance in Medicine publication. Unfortunately, polymerization of the DyDOTA-$(gly)_2$ and DyDOTA-$(gly)_3$ chelates proved to be extremely difficult, and only one version of the monomer chelates (DyDOTA) was successfully polymerized before the grant period ended. An alternate faster method could be to use dendrimers (n=16,32,64) instead of polymers to increase the total transverse relaxivity (r_2) per molecule. We have asked for a 6 month long EWOF to pursue this faster alternative approach that has more simplified chemistry.

15. SUBJECT TERMS
MRI Contrast Agent, T2 contrast, Prostate Cancer, PSMA Targeted Agent, Early Detection and Diagnosis, Dysprosium (Dy3+) Paramegnetic Chelate, T2-exchange

16. SECURITY CLASSIFICATION OF:			17. LIMITATION OF ABSTRACT	18. NUMBER OF PAGES	19a. NAME OF RESPONSIBLE PERSON
a. REPORT	b. ABSTRACT	c. THIS PAGE			USAMRMC
Unclassified	Unclassified	Unclassified	Unclassified	21	19b. TELEPHONE NUMBER *(include area code)*

Table of Contents

Page

1. INTRODUCTION

PC121497 Technical Abstract

The prostate-specific membrane antigen (PSMA), which is significantly over-expressed by prostate cancer cells, has proven to be an excellent target for imaging prostate cancer in mouse models, as recently shown for PSMA-targeted radiopharmaceuticals labeled with cysteineglutamate or lysine-glutamate ureas. Yet, dual-modality SPECT/CT and PET/CT imaging systems expose the subject to ionizing radiation, making them impractical for frequent therapeutic monitoring in patients. MRI systems offer superior anatomic resolution and soft tissue contrast compared to CT, making them an excellent tool for prostate cancer prevention studies. The effectiveness of MRI in the functional and molecular imaging regime is currently limited due to the lack of highly sensitive molecularly targeted contrast agents. Creating such agents would greatly improve the use of MRI for the early detection and diagnosis of prostate cancer. Our long-term goal is to use the newly described phenomena of T2-exchange to create targeted, highly sensitive, molecule-sized T2 agents for contrast-enhanced molecular imaging of prostate cancer with MRI. It was recently shown that lanthanide-based Ln3+DOTA chelates (Ln3+ = La, Gd, Lu) create enhanced negative contrast (i.e., darkening) in MRI through the chemical exchange of water molecules. The level of this "T2-exchange" contrast, which adds to the inherent paramagnetic T2 contrast of the Ln3+ ion, is proportional to the bound water molecule chemical shift and reaches a maximum at a specific water molecule exchange rate. It was also recently demonstrated that T2- exchange contrast could be increased by several orders of magnitude through simple linear polymerization of the Ln3+DOTA chelate. We hypothesize that by using these methods, a highly sensitive molecular imaging T2 contrast agent with a transverse relaxivity (r2) an order of magnitude greater than any currently existing contrast agent (e.g., SPIO) can be created, while retaining the advantages of using small molecules rather than nanoparticles for improved biological targeting, uptake, and clearing. These agents have the potential to accurately image the location and size of cancerous lesions within the prostate, and (through PSMA as a prognostic indicator) differentiate between indolent and aggressive forms, thereby performing disease staging entirely non-invasively. Also, in contrast to PET/CT or SPECT/CT, disease diagnostics and therapy monitoring would be performed on a single-modality MRI instrument without the risk of exposure to ionizing radiation. This would reduce patient stress by increasing specificity and early detection, simplifying the imaging protocol, and reducing scan time.

PC121497 Public Abstract

This research project will explore the idea of using a new chemical compound to help detect and image prostate cancer in the human body with magnetic resonance imaging (MRI). This method could allow prostate cancer to be detected at an earlier stage, determine it's exact location within the prostate, and possibly even determine what type of prostate cancer it is. The chemical compound (also known as an MRI "contrast agent") will be modified to attach itself to cancerous prostate cells but not to healthy prostate cells. In this way, the contrast agent would cause the cancer containing regions of the prostate to appear darker than the surrounding healthy tissue (that is, create "negative" contrast). This would allow the location of prostate cancer to be easily detected by

comparing MRI images from before and after administration of the intravenously injected contrast agent and looking for areas that appear darkened. This hypothesis will be tested by first evaluating both the contrast and cell-targeting capabilities of the contrast agent while outside the body (in vitro experiments), and then using mice bearing human prostate cancer tumors to evaluate the same capabilities when inside a body (in vivo experiments). If successful, this research could create a new class of highly sensitive, molecularly targeted MRI contrast agents for the early detection and diagnosis of prostate cancer. Also, in contrast to conventional PET/CT and SPECT/CT imaging, which use gamma rays and x-rays, MRI can be used for frequent therapeutic monitoring in patients without the harmful risks associated with ionizing radiation.

2. KEYWORDS

CT – x-ray computed tomography
DOTA – 1,4,7,10-tetraazacyclododecane-1,4,7,10-tetraacetic acid
Dy – Dysprosium
Gd – Gadolinium
Gly – Glycinate
La – Lanthanum
Ln – Lanthanide
Lu - Lutetium
MRI – Magnetic Resonance Imaging
PET – Positron Emission Tomography
PSMA – Prostate-Specific Membrane Antigen
r_2 – transverse relaxivity (sec-1mM-1)
SCID – severe combined immunodeficiency
SPECT – single photon emission computed tomography
SPIO – super paramagnetic iron oxide nanoparticle
T_2 – transverse relaxation time (sec)

3. ACCOMPLISHMENTS

- What were the major goals of the project?

From our Statement Of Work:

Task 1. Design and synthesis of a highly sensitive polymerized Dy3+DOTA-based T2 contrast agent (months 1-6):

1a. First, we will maximize the T2-exchange contrast generated by the Dy3+DOTA-based chelate by varying the water molecule exchange rate using several different DOTA sidearm structures (e.g., DOTA-, DOTA-(gly)2-, DOTA-(gly)4-). The maximum transverse relaxivity (r2) due to T2-exchange with a single Dy3+ ion is theoretically 16 sec-1mM-1. Dr. Wu will perform the chemical synthesis while Dr. Soesbe will perform the in vitro r2 analysis (months1-3).

1b. Once the ideal chemical structure/water molecule exchange rate has been determined, we will use the previously established polymerization method (3) to increase the level of T2 contrast by a factor of 20 to 100 times. If successful, the r2 from T2-exchange would then be 320 to 1600 sec-1mM-1 per molecule. Dr. Wu will perform the chemical synthesis while Dr. Soesbe will perform the in vitro r2 analysis (months 4-6).

Task 2. Create targeted versions of the polymerized T2 contrast agent and evaluate cell receptor binding characteristics with in vivo and in vitro experiments (months 6-12):

2a. We will create targeted versions of the of the polymerized T2-exchange contrast agent by attaching molecular targeting groups along the backbone of the linear polymer chain. One version will be labeled with biotin (for in vitro binding to streptavidin) while another version will be labeled with cysteine-glutamate or lysine-glutamate ureas (for in vivo binding to the prostate specific membrane antigen, or PSMA) (5). Dr. Wu will perform the chemical synthesis and analysis (months 6-8).

2b. The detection limit (and thus the sensitivity) of the targeted low molecular weight T2 contrast agent will me measured in vitro using the biotin labeled version of the polymer. A concentration array will be created using a small well plate, where each well will contain the same number of streptavidin coated agarose beads and the receptor concentration on the bead surface is precisely known. The level of T2 contrast in each well will be imaged using a small animal 9.4 T MRI system. Dr. Soesbe will perform the in vitro set up, MR imaging, and analysis (months 9-10).

2c. In vivo prostate cancer cell receptor binding will be evaluated using the cysteine-glutamate or lysine-glutamate urea labeled version of the polymer. The tumor uptake characteristics will be assessed by injecting the agent into SCID mice (8 total) bearing PSMA+ flank tumor xenografts (e.g., PC3-PIP) (1). The mice will then be imaged on a 9.4 T MRI system. The specificity and selectivity will be measured by using PSMA- xenografts (e.g., PC3-flu) within in the same mouse and by injecting the mice with a PSMA blocker (e.g., 2-(phosphonomethyl)pentanedioic acid) before administration of the contrast agent. Facility research staff will perform the tumor implantation while Dr. Soesbe will perform all in vivo imaging (months 11-12).

- What was accomplished under these goals?

Task 1a. : Completed (3 months total)

Four different versions of the DyDOTA-based chelate were synthesized (DyDOTA, DyDOTA-$(gly)_2$, DyDOTA-$(gly)_3$, and DyDOTA-$(gly)_4$). Each chelate had a different number of glycinate (gly) side-arms (i.e., 0, 2, 3, or 4) and thus different water molecule exchange rates. Since T_2-exchange is dependent on the water molecule exchange rate, each chelate had a different transverse relaxivity (r_2) value. The non-water molecule exchanging chelate DyTETA was also synthesized in order to measure the transverse relaxivity (r_2) due to the presence of the paramagnetic Dy3+ ion itself (i.e., outer sphere relaxation). Both the transverse relaxivities (r_2) and the water molecule exchange rates for

the five Dy3+ chelates were measured in vitro on a vertical 400 MHz NMR system. These data were in excellent agreement with the theoretical values predicted by the Swift-Connick theory, proving this part of our hypothesis to be correct. These data showed that (at 9.4 T and 37 degrees Celsius) the water molecule exchange rate for DyDOTA was too fast, and that DyDOTA-$(gly)_4$ was too slow, but that both DyDOTA-$(gly)_2$ and DyDOTA-$(gly)_3$ had exchange rates that placed them close to the maximum r_2 value. Therefore, DyDOTA-$(gly)_2$ and DyDOTA-$(gly)_3$ were selected as candidates for polymerization. Further details for this completed task (including *in vitro* images) can be found in our Magnetic Resonance in Medicine publication, which is included in the Appendix at the end of this report.

Task 1b. : Attempted, but not completed (9 months, estimated time was 3 months)

At project month 4 we started synthesizing the polymers, but polymerization of the DyDOTA-$(gly)_2$ and DyDOTA-$(gly)_3$ chelates proved to be far more challenging than initially anticipated. Under the guidance of Dr. Yunkou Wu (Faculty), Lei Zhang (Undergraduate Research Assistant) attempted to synthesize the polymers. He found difficulty in producing the final compounds due to the incompatibility of our synthetic methods with the stability of the polymer. When we attempted the polymerization with the mettalated monomers, we found that solubility issues limited our polymerization efficiency. This was due to the charge on the monomer being highly cationic. When we then used the organic framework *without* the lanthanide ion during polymerization, we were successful and resulted in a high efficiency of polymerization (up to ~100 units). Unfortunately, during subsequent mettalation of the of the ~100 unit organic polymer we observed cleavage of the peptide backbone due to the acidity of the lanthanide ions and their kinetic affinity to carbonyls. In other words, the polymer backbone fell apart. This was apparent as chemical analysis observed a series of lower molecular weight molecules that were consistent with degradation of a larger molecular weight polymer. We were able to overcome this degradation (by Dr. Wu, see below) with the addition of citrate during mettalation, which was used to limit the kinetically favorable chelation along the backbone and to allow for the thermodynamically favorable chelation by the macrocycle unit.

At project month 11 (December 2014), Mr. Zhang stopped working on this research project and all polymerization attempts were continued by Dr. Yunkou Wu directly. By using Lei Zhang's starting materials, Dr. Wu was able to synthesize the DyDOTA version of the polymer within two weeks time. Initial characterization showed the polymer backbone length to be approximately 100 units with about 50% population of DyDOTA. Therefore the transverse relaxivity (r_2) of this molecule should be 50 times that of the monomer chelate. While the water molecule exchange rate of DyDOTA is not ideal (too fast) for maximizing T_2-exchange at 9.4 T and 37 degrees Celsius, this nonetheless proved that polymerization of the DyDOTA-based chelates was indeed possible. At project month 12 two things happened 1) Our Lead Chemist Dr. Wu left UT Southwestern, and 2) our 12-month long grant period was up. Therefore no further chemistry was completed on this project.

After speaking with Dr. Mark Milne (Postdoctoral researcher) we decided to ask for a 6 to 12-month long EWOF to complete Task 1b as well as some aspects of Task 2 (specifically *in vitro* and *in vivo* imaging of the non-targeted agent). Since polymerization of the remaining DyDOTA-based chelates would require synthesizing new starting materials, and since Dr. Wu (our polymerization expert) is no longer at our institution, we have decided to use dendrimers to create multiple DyDOTA-based molecules instead of polymers. This will greatly simplify the required chemistry as the dendrimer backbones (n = 32, 64, 128) can be simply purchased (e.g., from Sigma Aldrich). Also, substituting dendrimers for polymers does not change the research goals of our initial Statement Of Work (SOW). During the proposed EWOF we will create DyDOTA-$(gly)_2$ and DyDOTA-$(gly)_3$ dendrimers (n = 64), perform in vitro characterization and imaging, and initial in vivo imaging. Since the dendrimers will be non-targeted, we can use the collection by the mouse kidneys to determine the *in vivo* T_2-exchange contrast capabilities, similar to our previous publications.

Task 2a, 2d, and 2c: Not completed
Since these tasks depended on successful polymerization of the monomer chelates, which took much longer than expected (> 9 months), they could not be completed in time

- What opportunities for training and professional development have the project provided?

Todd C. Soesbe, Ph.D.
Training: Dr. Soesbe had to learn O-17 NMR spectroscopy and Matlab fitting in order to measure the water molecule exchange rates of the DyDOTA-based monomers.
Professional Development: Dr. Soesbe held bi-weekly lab group meetings to help with collaboration among the group members. He also gave two conference presentations (see Section 6) about this research where his discussed similar research with peers.

Yunkou Wu, Ph.D.
Training: Dr. Wu received training on how to operate the Agilent 9.4 T animal MRI system from Dr. Soesbe.
Professional Development: Dr. Wu attended the bi-weekly lab group meetings to discuss aspects of the current project, present results, and review current and previous literature.

Mark Milne, Ph.D.
Training: Dr. Milne received training from Dr. Wu on polymer chemistry and synthesis methods. He also received training from Dr. Ratnakar on dendrimer chemistry and synthesis.
Professional Development: Dr. Milne attended the bi-weekly lab group meetings to discuss aspects of the current project, present results, and review current and previous literature.

Lei Zhang

Training: Mr. Zhang received training from Dr. Wu on polymer chemistry and synthesis methods.
Professional Development: Mr. Zhang attended the bi-weekly lab group meetings to discuss aspects of the current project, present results, and review current and previous literature.

- How were the results disseminated to the community of interest?
Along with our Magnetic Resonance in Medicine publication, Dr. Soesbe presented these data at several conferences for peer evaluation and education. He also used these data to discuss "current exciting research" when making presentations at UT Southwestern to summer undergraduate research students and teachers (i.e., the UT Southwestern SURF and STARS programs) and to graduate school candidates for the UT Southwestern Biomedical Engineering graduate program.

- What do you plan to do during the next reporting period to accomplish the goals?

Nothing to report, as this is the Final Report.

4. IMPACT

- What was the impact on the development of the principal discipline(s) of the project?

Although T_2 contrast by T_2-exchange has existed in NMR and MRI for over 30 years, until our research, no one has truly understood the dependence on proton exchange either through –NH and –OH bonds or H_2O exchange. Also, until our research, no one has ever attempted to maximize paramagnetic T_2-exchange by modulating the water molecule exchange rate using chelate structure. Our success with the monomer DyDOTA-based chelates (as described in our MRM publication, see Appendix) opens up a new modality for generating T_2 contrast in magnetic resonance imaging. T_2-exchange differs from conventional T_2^* contrast mechanisms (such as super-paramagnetic iron oxide nanoparticles, i.e. SPIO) in that it does not rely on magnetic susceptibility to shorten T_2 times. Therefore, susceptibility-based image artifacts are non-existent with T_2-exchange contrast agents. Also, when compared to SPIO, polymerized or dendrimerized T_2-exchange contrast agents are molecule-sized and not nanoparticle sized. This enhances the potential application of T_2-exchange contrast agents for molecular imaging in MRI, where effective agent uptake and targeting are crucial. Since our 2014 publication, there has already been another T_2-exchange publication in MRM by another group (NH Yadav, et al., Magn Reson Med, 72:823-828, 2014) describing the use of D-Glucose as a diamagnetic T_2-exchange agent, as well as another groups T_2-exchange publication that is currently in review by Magnetic Resonance in Medicine. It is anticipated that T_2-exchange contrast will become an important tool for contrast-enhanced imaging with magnetic resonance.

- What was the impact on other disciplines?

Nothing to report.

- What was the impact on technology transfer?

Nothing to report.

- What was the impact on society beyond science and technology?

Nothing to report.

5. CHANGES/PROBLEMS

- Changes in approach and reasons for change.

Although polymerization of the DyDOTA-based chelates was shown to be possible, it was also very time consuming and greatly inhibited our progress for this 12-month long grant. As an alternate approach we have suggested using a dendrimers structure (n = 32, 64, or 128) for the multiple DyDOTA chelate backbone. Since dendrimer backbones can simple be purchased (e.g., Sigma Aldrich), this will greatly simplify the chemistry required for synthesis, and greatly speed up the project, without changing the overall goals of our Statement of Work. We have suggested this path for our applied EWOF.

- Actual or anticipated problems or delays and actions or plans to resolve them.

Please see previous statement.

6. PRODUCTS

- Peer-Reviewed Journal Publications (see Appendix for full article copy)

Authors: Todd C. Soesbe, S. James Ratnakar, Mark Milne, Shanrong Zhang, Quyen N. Do, Zoltan Kovacs, and A. Dean Sherry
Title: Maximizing T2-exchange in Dy3+DOTA-(amide)x chelates: fine-tuning the water molecule exchange rate for enhanced T2 contrast in MRI
Journal: Magnetic Resonance in Medicine
Volume: 71
Date: March 2014
Page numbers: 1179-1185
Status of publication: published
Acknowledgment of federal support: yes

- Peer-Reviewed Conference Presentations (see Appendix for abstract copies)

Date: April 3, 2014
Presenter: Todd C. Soesbe, Ph.D.
Presentation type: Oral

Presentation title: Contrast, paramagnetism, and their applications in MRI
Host: UT Southwestern Medical Center at Dallas and The University of Texas at Dallas Joint Biomedical Engineering Graduate Program, Retreat & Scientific Symposium
Location: Dallas, Texas

Date: November 8, 2014
Presenter: Todd C. Soesbe, Ph.D.
Collaborators: James Ratnakar, Mark Milne, Fiemu Nwariaku, A. Dean Sherry, and Robert E. Lenkinski
Presentation type: Oral
Presentation title: Advancing the early detection and diagnosis of primary and recurring thyroid cancers using a molecularly targeted T2-exchange MRI contrast agent
Host: International Society of Magnetic Resonance in Medicine, Workshop Series 2014: Magnetic resonance in cancer: challenges and unmet needs
Location: Austin, Texas

7. PARTICIPANTS & OTHER COLLABORATING ORGANIZATIONS

- What individuals have worked on the project?

Name: Todd C. Soesbe, Ph.D. (Principal Investigator)
Project role: Faculty, Physicist and MR Imaging Specialist
Researcher identifier (UT Southwestern ID): 56841
Nearest person month worked: 6
Contribution to project: Dr. Soesbe served as Principal Investigator for this project by organizing and driving the research and performing all imaging experiments.
Funding support: UT Southwestern Medical Center

Name: Yunkou Wu, Ph.D.
Project role: Faculty, Lead Chemist
Researcher identifier (UT Southwestern ID): 121991
Nearest person month worked: 3
Contribution to project: Dr. Wu served as the principal chemist for this project and was responsible for synthesis, polymerization, and characterization of the Dy3+DOTA-based ligands.
Funding support: UT Southwestern Medical Center

Name: Mark Milne, Ph.D.
Project role: Postdoctoral Researcher, Chemist
Researcher identifier (UT Southwestern ID): 145045
Nearest person month worked: 1
Contribution to project: Dr. Milne assisted Dr. Wu with the synthesis and polymerization of the Dy3+DOTA-based ligands and will be responsible for synthesizing the dendrimers version of the Dy3+DOTA chelates during the requested EWOF.
Funding support: UT Southwestern Medical Center

Name: Lei Zhang
Project role: Undergraduate Research Assistant, Chemist
Researcher identifier (UT Southwestern ID): 133372
Nearest person month worked: 2
Contribution to project: Mr. Zhang assisted Dr. Wu with the synthesis and polymerization of the Dy3+DOTA-based ligands.
Funding support: The University of Texas at Dallas

- Has there been a change in the active other support of the PD/PI(s) or senior/key personnel since the last reporting period?

Nothing to report.

- What other organization were involved as partners?

Nothing to report.

8. SPECIAL REPORTING REQUIREMENTS

Nothing to report.

9. APPENDECIES

- MRM publication
- ISMRM cancer workshop abstract

PRECLINICAL AND CLINICAL IMAGING – Rapid Communication

Magnetic Resonance in Medicine 71:1179–1185 (2014)

Maximizing T_2-Exchange in Dy^{3+}DOTA-(amide)$_X$ Chelates: Fine-Tuning the Water Molecule Exchange Rate for Enhanced T_2 Contrast in MRI

Todd C. Soesbe,[1,2]* S. James Ratnakar,[1] Mark Milne,[3] Shanrong Zhang,[1] Quyen N. Do,[4] Zoltan Kovacs,[1,4] and A. Dean Sherry[1,2,4]

Purpose: The water molecule exchange rates in a series of DyDOTA-(amide)$_X$ chelates were fine-tuned to maximize the effects of T_2-exchange line broadening and improve T_2 contrast.
Methods: Four DyDOTA-(amide)$_X$ chelates having a variable number of glycinate side-arms were prepared and characterized as T_2-exchange agents. The nonexchanging DyTETA chelate was also used to measure the bulk water T_2 reduction due solely to T_2^*. The total transverse relaxivity (r_{2tot}) at 22, 37, and 52°C for each chelate was measured in vitro at 9.4 Tesla (400 MHz) by fitting plots of total T_2^{-1} versus concentration. The water molecule exchange rates for each complex were measured by fitting ^{17}O line-width versus temperature data taken at 9.4 Tesla (54.3 MHz).
Results: The measured transverse relaxivities due to water molecule exchange (r_{2ex}) and bound water lifetimes (τ_M) were in excellent agreement with Swift-Connick theory, with DyDOTA-(gly)$_3$ giving the largest $r_{2ex} = 11.8\ s^{-1}\ mM^{-1}$ at 37°C.
Conclusion: By fine-tuning the water molecule exchange rate at 37°C, the transverse relaxivity has been increased by 2 to 30 times compared with previously studied Dy^{3+}-based chelates. Polymerization or dendrimerization of the optimal chelate could yield a highly sensitive, molecule-sized T_2 contrast agent for improved molecular imaging applications. **Magn Reson Med 71:1179–1185, 2014. © 2014 Wiley Periodicals, Inc.**

Key words: MRI; T_2 contrast; T_2-exchange; water molecule exchange; in vitro; Dysprosium(III)

INTRODUCTION

Contrast in MR Imaging

MRI can be used to create a three-dimensional image representing the water proton (^1H) density within a subject (1,2). Because the human body is approximately 70% water, most tissues have a sufficiently large water proton signal to allow for high-resolution anatomical imaging. The contrast between different soft tissue types, which results in some tissues appearing brighter or darker than others, depends upon both the endogenous proton density and the T_1 and T_2 relaxation times (3). MRI tissue contrast can be further enhanced by introducing an exogenous contrast agent (4). These agents shorten the endogenous T_1 and T_2 relaxation times of tissue water to enhance the contrast and highlight specific anatomic features or dynamic processes.

The most widely used MRI contrast agents consist of various chelated forms of Gd^{3+} where the central ion is surrounded by a multidentate ligand that typically occupies eight of nine possible coordination positions (5,6). Gd^{3+} is most effective at relaxing water protons because this ion has seven unpaired electrons distributed isotropically in the 4f orbitals ($^8S_{7/2}$) and an electron relaxation rate that is approximately 10^6 times slower than any other lanthanide ion (7). This reduced electron relaxation rate is more in tune with the typical Larmor frequencies of ^1H protons in MRI ($\omega = \gamma B_o$) and, therefore, enhances the mechanism of electron to proton dipole-dipole relaxation (8). The relaxation efficiency of Gd^{3+} also depends upon the rapid chemical exchange of water molecules between a single inner-sphere coordination position of Gd^{3+} ion and bulk water. Although Gd^{3+} shortens both the T_1 and T_2 of water protons, the T_1 effects are more pronounced because the T_1 of tissue water protons are approximately an order of magnitude longer than T_2. Hence, for most common imaging sequences, a typical clinical dose of Gd^{3+} agent (e.g., 0.1 mmol/kg) will cause tissue regions of uptake to appear brighter than the surrounding tissue. Nonetheless, the effects of T_2 shortening (image darkening) can be observed in tissues (such as the kidneys) where Gd^{3+} accumulates in high concentrations.

Other lanthanide ions such as Tb^{3+}, Dy^{3+}, and Ho^{3+} have fewer unpaired electrons distributed anisotropically in the 4f orbitals and relatively rapid electron relaxation rates compared with Gd^{3+}. These faster rates, combined with larger

[1]Advanced Imaging Research Center, UT Southwestern Medical Center, Dallas, Texas, USA.
[2]Department of Radiology, UT Southwestern Medical Center, Dallas, Texas, USA.
[3]Department of Chemistry, University of Western Ontario, London, Ontario, Canada.
[4]Department of Chemistry, University of Texas, Dallas, Texas, USA.
Grant sponsor: National Institutes of Health; Grant number: CA-115531, CA-126608: EB-004582; Grant sponsor: Robert A. Welch Foundation; Grant number: AT-584.
*Correspondence to: Todd C. Soesbe, Ph.D., Advanced Imaging Research Center, University of Texas Southwestern Medical Center, 5323 Harry Hines Boulevard, Dallas, TX 75390-8568. E-mail: todd.soesbe@utsouthwestern.edu
Additional Supporting Information may be found in the online version of this article.
Received 20 August 2013; revised 24 November 2013; accepted 2 December 2013
DOI 10.1002/mrm.25091
Published online 3 January 2014 in Wiley Online Library (wileyonlinelibrary.com).

magnetic moments (7), make these ions more effective as T_2^* agents. This susceptibility-based T_2 relaxation mechanism is due to the magnetic moments of the Ln^{3+} ions causing local B_o inhomogeneities in their immediate vicinity ($\approx$15 Å diameter) (7). Water molecule protons either directly bound to the Ln^{3+} ion (i.e., inner-sphere relaxation) or within the vicinity of the Ln^{3+} ion (i.e., outer-sphere relaxation) experience an altered B_o field and precess at a different Larmor frequency ($\omega = \gamma(B_o \pm \Delta B)$). These different Larmor frequencies result in increased spin de-phasing in the plane transverse to B_o and thus shorter effective T_2 times. In this way, certain paramagnetic chelates can act as susceptibility or T_2^* agents in a manner similar to superparamagnetic iron oxide nanoparticles (9). Furthermore, unlike Gd^{3+}, the remaining paramagnetic lanthanides ions can induce large hyperfine shifts in all chelate protons including those in exchange with water protons (i.e., −NH and −OH protons and any inner-sphere water molecules) (10–12). This hyperfine shift ($\Delta\omega$) has lead to the development of two relatively new MRI contrast mechanisms: chemical exchange saturation transfer (CEST) (13) and T_2-exchange (T_{2ex}). While the former has been recently reviewed in depth elsewhere (14,15), the latter is discussed in more detail in the following section.

T_2-exchange Theory and Background

It was recently shown that the same intermediate water molecule exchange rates that facilitate paramagnetic chemical exchange saturation transfer (paraCEST) (16) between the inner-sphere of EuDOTA-(amide)$_4$ chelates and bulk water can also significantly reduce the bulk water T_2 through a T_{2ex} mechanism (17). The T_{2ex} contribution of these Eu^{3+}-based agents can be quite substantial even though the Eu^{3+} ion is only weakly paramagnetic (18). T_{2ex} is caused by mobile proton exchange between the chelate and the bulk water. This proton exchange can occur through exchangeable −NH and −OH protons on the ligand and through water molecule exchange with the inner-sphere of the Ln^{3+} ion. The T_{2ex} mechanism, which is independent of the CEST saturation pulse, is a function of the agent concentration (mM), the number of proton or water molecule exchange sites (q), the bound proton chemical shift ($\Delta\omega$), and most importantly the proton or water molecule exchange rates (k_{ex}). It has also been shown that the transverse relaxivity caused by T_{2ex} (i.e., r_{2ex}) reaches a peak value for a given B_o at a specific exchange rate defined by $k_{ex} = \Delta\omega$, where $\Delta\omega$ is expressed in rad s^{-1} (17,19,20).

Diamagnetic T_{2ex} from compounds with exchanging −NH or −OH protons (e.g., NH_4Cl) has long been used for bulk water solvent signal suppression in high-resolution NMR experiments (21,22), and has more recently been proposed as an exogenous T_2 contrast mechanism for MRI (23,24). However, diamagnetic T_{2ex} agents require high concentrations (e.g., 500 mM) to achieve significant bulk water T_2 reduction and negative contrast, making them impractical for in vivo applications. The T_{2ex} effect can be greatly increased by using inner-sphere water molecule exchange in chelates containing paramagnetic Ln^{3+} ions. This was originally demonstrated by Aime et al (25) where it was shown that the amount of DyDOTA-(mono-amide) required to suppress the bulk water peak in high-resolution NMR experiments was reduced by a factor of 200 (from 500 mM to 2.5 mM). This increase in T_{2ex} sensitivity is mainly due to the increase in $\Delta\omega$ when moving from diamagnetic −NH and −OH proton exchange (where $\Delta\omega$ is typically 2 to 5 ppm) to paramagnetic Ln^{3+} inner-sphere water molecule exchange (where $\Delta\omega$ can range from 50 ppm for Eu^{3+} to 800 ppm for Dy^{3+}) (11). It is important to note that the reduction in the bulk water T_2 due to T_{2ex} is *in addition* to the paramagnetic line broadening caused by the Ln^{3+} ion itself (T_{2para}). This makes some of the Ln^{3+} ions (most notably Dy^{3+}) strong candidates for development into highly sensitive T_2 contrast agents for MRI.

In fact, some chelates containing the Dy^{3+} ion have previously been pursued as T_2 contrast agents. The most well-known example being DyDTPA-BMA or Sprodiamide™ (Nycomed, UK) (26), the Dy^{3+} analog of the nonionic GdDTPA-BMA or gadodiamide (i.e., Omniscan™; Nycomed, UK). DyDTPA-BMA was first assessed for demarcation of myocardial ischemia (26–30), tumor tissue characterization (31), and even Phase I clinical trials for cerebral perfusion imaging (32). These in vivo examples illustrate the many possible applications for a small molecule-sized T_2 MRI contrast agent. Other previous Dy^{3+}-based chelate studies include DyDTPA-based derivatives and starch microparticles (19,33,34), DyDOTA-based monomers and dendrimers (25,33,35), and the MS-325 human serum albumin binding ligand (20). It is important to note that for these previous Dy^{3+} chelates the water molecule exchange rates at 37°C were either too fast or too slow to maximize r_{2ex}, typically being one to two orders of magnitude away from the ideal exchange rate defined by $k_{ex} = \Delta\omega$ (19,33). Interestingly, several of the early studies on Dy^{3+} chelates did observe that their total transverse relaxivity (r_{2tot}) was indeed proportional to the water molecule exchange rate (k_{ex}) and bound water chemical shift ($\Delta\omega$). This was demonstrated by varying the chemical structure, temperature, and B_o field (19,20,25,33), and was elegantly explained in theoretical detail by Caravan et al (20). Although the concept of maximizing the transverse relaxivity for a Dy^{3+}-based chelate by adjusting the water molecule exchange to the ideal rate had been proposed, to the best of our knowledge it has not been previously implemented.

Hypothesis and Objectives

In this study, Swift-Connick theory (17,19,20) was used to optimize the transverse relaxivity produced by a series of DyDOTA-(amide)$_X$ systems at 37°C. This was achieved by modulating the water molecule exchange rate with different DOTA ligand side-arm structures, and by maximizing $\Delta\omega$ with magnetic field strength ($B_o = 9.4$ Tesla [T]). The DyDOTA-(amide)$_X$ chelate structure that gave the ideal exchange rate at 400 MHz (9.4T) and 37°C was determined by in vitro T_2 measurements, and the water molecule exchange rates for each chelate were confirmed using variable temperature ^{17}O line-width measurements. Based on these results, one can hypothesize that polymerized or dendrimerized versions of these DyDOTA-(amide)$_X$ chelates could create a new class of highly sensitive T_2 contrast agents for MRI.

METHODS

Chelate Synthesis

Five different Dy^{3+} chelates were synthesized (Fig. 1), each having a different water molecule exchange rate. Four of the chelates (a–d) used the DOTA ligand (1,4,7,10-tetraazacyclododecane-1,4,7,10-tetraacetic acid) and one (e) used the

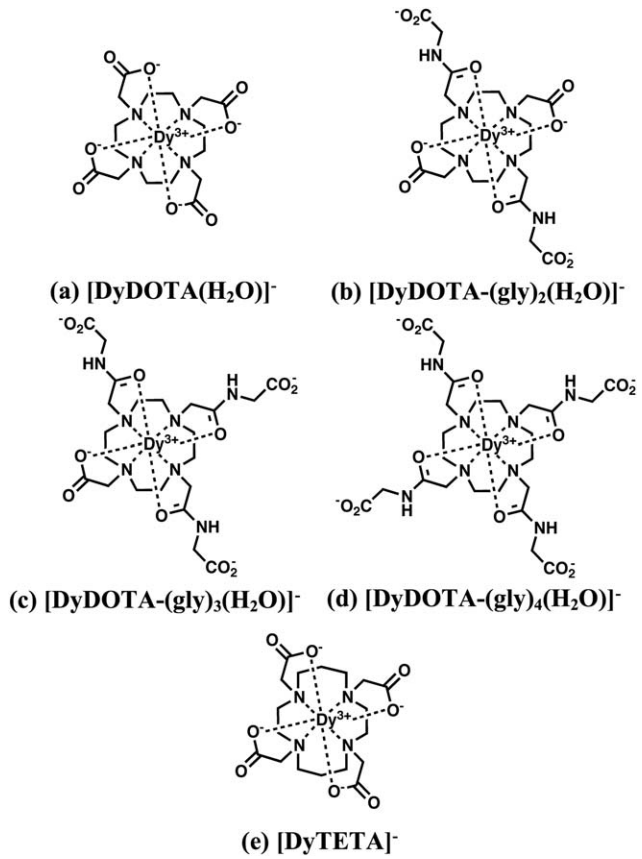

FIG. 1. Chemical structures of the five Dy^{3+} chelates used in this study. The four DyDOTA-(amide)$_X$ chelates (**a–d**) have varying inner-sphere water molecule exchange rates, while the DyTETA chelate (**e**) has no water molecule exchange and therefore no T_{2ex} effects on the bulk water T_2.

TETA ligand (1,4,8,11-tetraazacyclotetradecane-1,4,8,11-tetraacetate). The four DOTA-(amide)$_X$ ligands were synthesized according to earlier published methods (36–38), while the TETA ligand was purchased from Sigma-Aldrich (St. Louis, MO). All five Dy^{3+} complexes were prepared by reacting the corresponding free ligand with $DyCl_3$ in water at pH 6.0 and 25°C for 24 h. The absence of any free Dy^{3+} metal was confirmed using the Xylenol Orange indicator test, and the concentration of Dy^{3+} in each complex was measured using ICP-OES analysis.

The water molecule exchange rates of the four DOTA-(amide)$_X$ chelates were inversely proportional to the number glycinate side-arm structures ($NHCH_2COO^-$) attached to the DOTA ring (i.e., 0, 2, 3, or 4). Therefore, the water molecule exchange rate ranged from fast for DyDOTA, to slower with additional glycinate amide groups, to slowest for DyDOTA-(gly)$_4$. The DyTETA chelate, while structurally similar to DyDOTA, lacks an inner-sphere water molecule and cannot by definition have a T_{2ex} contribution to the water line-width. Hence, this chelate served as a useful control to measure the changes in the bulk water T_2 due solely to the paramagnetic effects of the Dy^{3+} ion (i.e., outer-sphere relaxation only).

In Vitro Experiments

The total transverse relaxivity (r_{2tot}) was measured as a function of temperature for each of the five Dy^{3+} chelates. This was performed by creating a concentration array for each chelate (0.125, 0.25, 0.5, and 1.0 mM) in 5 mm NMR tubes, with each sample adjusted to a pH of 7.0. The total T_2 (T_{2tot}) for each sample was then measured on an Agilent (Santa Clara, CA) 400 MHz NMR system using the Carr-Purcell-Meiboom-Gill pulse sequence. The T_{2tot} data were acquired at 22, 37, and 52°C for each chelate to determine how the r_{2tot} varied as a function of water molecule exchange rate. The r_{2tot} values (in units of s^{-1} mM^{-1}) were calculated by plotting T_{2tot}^{-1} versus Dy^{3+} concentration and using the slope of the least squares fitted line. The transverse relaxivity due to water molecule exchange (r_{2ex}) for each DyDOTA-(amide)$_X$ chelate was then calculated by subtracting the total transverse relaxivity of DyTETA from r_{2tot} (i.e., $r_{2ex} = r_{2tot} - r_{2DyTETA}$) at each temperature. The measurement error in r_{2tot} from the least squares fitting was less than 10% and the Dy^{3+} concentration of each sample was verified by ICP-OES analysis.

The water molecule exchange rate for each Dy^{3+} chelate was calculated by measuring the variation in the ^{17}O peak line-width as a function of temperature. Aqueous samples of each chelate (18 mM [Dy^{3+}], pH 7.0, and enriched to 2% ^{17}O) were loaded into 18 μL spherical capillaries from Wilmad-LabGlass (Vineland, NJ) to remove any susceptibility effects and then placed inside thin-walled, water-filled 5 mm NMR tubes also from Wilmad-LabGlass. An Agilent 400 MHz NMR system was used to measure the ^{17}O line-width (TR = 250 ms, acquisition time = 80 ms, 128 averages) as the temperature was varied from 5 to 90°C in 5°C steps (18 points). The change in transverse relaxation rate due to exchange (T_{2ex}^{-1}) as a function of temperature (i.e., water molecule exchange rate) was calculated by first converting the line-width data ($T_{2tot}^{-1} = \pi \times$ line-width) then subtracting the DyTETA data ($T_{2ex}^{-1} = T_{2tot}^{-1} - T_{2DyTETA}^{-1}$). The water molecule exchange rates were then calculated by fitting the temperature dependant T_{2ex}^{-1} data with a model given by Pubanz et al (39) and the MATLAB nonlinear least squared algorithm (Natick, MA). The measurement error in τ_M (± one standard deviation) was estimated to be less than 20%.

In vitro images of the five Dy^{3+} chelate samples, along with a pure water standard, were acquired simultaneously on an Agilent (Santa Clara, CA) 9.4T (400 MHz) small animal MRI system using standard 5 mm diameter HPLC glass tubes and a 38 mm diameter ^1H birdcage volume coil. Each sample was approximately 200 μL with a Dy^{3+} concentration of 20 mM and a pH of 7.0. The sample temperature was monitored with a thermocouple and held constant by a heated air system from Small Animal Instruments (Stony Brook, NY). The fast spin-echo settings were: TR/TE = 2500/12.4 ms, echo train = 8, averages = 8, field of view = 64 × 16 × 5 mm, matrix = 512 × 128 × 1 pixels, with an image scan time of 5 m 25 s.

RESULTS

In Vitro Results

A plot of T_{2tot}^{-1} versus Dy^{3+} concentration is shown in Figure 2 for DyDOTA-(gly)$_2$ at 22, 37, and 52°C. The slope of each least squares fitted line gives the calculated r_{2tot} at that temperature. Figure 2 shows that r_{2tot}

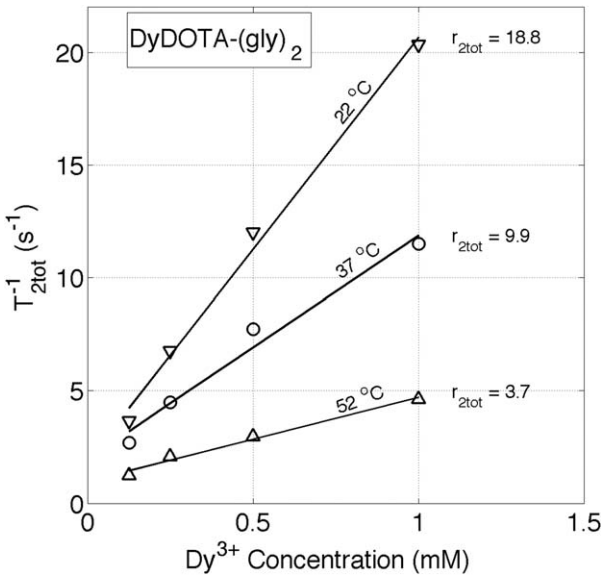

FIG. 2. A plot of total transverse relaxation rate (T_{2tot}^{-1}) versus Dy^{3+} concentration for the DyDOTA-$(gly)_2$ chelate at 22, 37, and 52°C. The slope of the least square fitted lines gives the total transverse relaxivity (r_{2tot}) at that temperature. Measurement error for r_{2tot} was less than 10%.

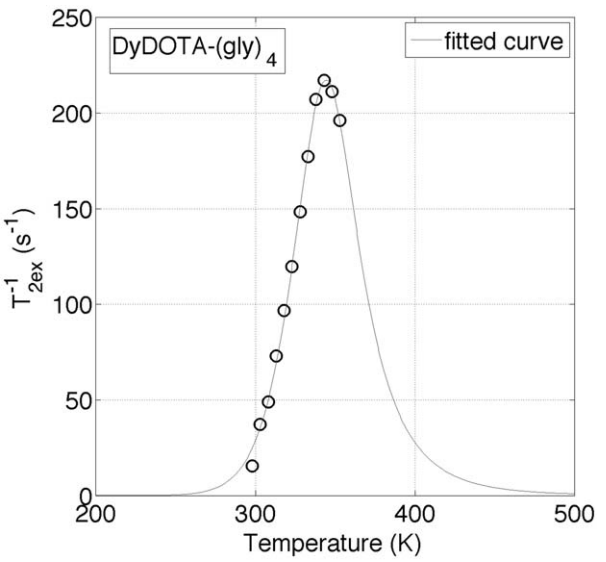

FIG. 3. A plot of the ^{17}O measured exchange transverse relaxation rate (T_{2ex}^{-1}) versus temperature for the DyDOTA-$(gly)_4$ chelate. The least squares fit to the data (line) allows the water molecule exchange rate at 37°C to be calculated (39).

decreases with increasing temperature indicating that, within this temperature range, slower water molecule exchange rates (k_{ex}) give higher total relaxivity values for DyDOTA-$(gly)_2$. The similarly measured r_{2tot} values for all five Dy^{3+} chelates studied are summarized in Table 1, which also shows the calculated r_{2ex} values (i.e., $r_{2ex} = r_{2tot} - r_{2DyTETA}$) for each temperature. Table 1 shows that over the given temperature range, r_{2tot} and r_{2ex} are inversely proportional to temperature for DyDOTA and DyDOTA-$(gly)_2$ yet are proportional to temperature for DyDOTA-$(gly)_3$ and DyDOTA-$(gly)_4$. Note that for DyTETA, which has no water molecule exchange, the r_{2tot} is relatively independent of temperature. Also included in Table 1 are the bound water lifetimes ($\tau_M = k_{ex}^{-1}$) at 22, 37, and 52°C that were calculated from the variable-temperature ^{17}O data. Figure 3 shows a plot of the ^{17}O measured T_{2ex}^{-1} versus temperature for DyDOTA-$(gly)_4$ (raw data shown as circles). The Matlab fit to these data, based on Eq. [1] in Pubanz et al (39), gave values for k_{ex}^{298} and $\Delta H^{\pm}$ which were used to calculate τ_M at each temperature using the equation below:

$$\tau_M^{-1} = \frac{k_{ex}^{298} T}{298.15} \exp\left[\frac{\Delta H^{\pm}}{R}\left(\frac{1}{298.15} - \frac{1}{T}\right)\right] \quad [1]$$

where k_{ex}^{298} is the water molecule exchange rate at 25°C, T is temperature in Kelvin, $\Delta H^{\pm}$ is the enthalpy of activation, and R is the universal gas constant. Similar fits were performed for the other DyDOTA-$(amide)_X$ chelates. A full description of the ^{17}O methods and Matlab fit can be found in the Supplementary Material.

The data from Table 1 can be more easily interpreted using a Swift-Connick plot (17) for Dy^{3+} at 400 MHz (9.4T) as shown in Figure 4. Swift-Connick theory (21) predicts that the transverse relaxivity due to water molecule exchange (r_{2ex}) is a function of the bound water molecule lifetime (τ_M) as given by:

$$r_{2ex} = (1.8 \times 10^{-5}) \frac{\tau_M \Delta\omega^2}{1 + \tau_M^2 \Delta\omega^2} \quad [2]$$

where $\Delta\omega$ is the paramagnetic frequency shift of the bound water molecule protons expressed in rad s^{-1} (17,40). Equation [2] predicts that for Dy^{3+} at 9.4T (using $\Delta\omega = -730$ ppm or 1.835×10^6 rad s^{-1}) the r_{2ex} will

Table 1
Measured r_{2tot} and r_{2ex} Values for the Five Dy^{3+} Chelates Taken at Three Different Temperatures, Where $r_{2ex} = r_{2tot} - r_{2DyTETA}$[a]

	Total transverse relaxivity r_{2tot} (s^{-1} mM^{-1})			Exchange transverse relaxivity r_{2ex} (s^{-1} mM^{-1})			Bound water molecule lifetime τ_M (ns)		
Dy^{3+} chelate	52°C	37°C	22°C	52°C	37°C	22°C	52°C	37°C	22°C
DyDOTA	0.17	0.43	1.5	0.01	0.22	1.3	0.8	3.7	22
DyDOTA-$(gly)_2$	3.7	9.9	18.8	3.6	9.7	18.6	93	190	400
DyDOTA-$(gly)_3$	13.2	12.0	4.2	13.0	11.8	3.9	330	1,800	7,700
DyDOTA-$(gly)_4$	8.6	3.6	1.4	8.5	3.4	1.2	1,800	4,900	14,000
DyTETA	0.16	0.21	0.22	(no water molecule exchange)					

[a]Also shown are the variable-temperature ^{17}O measured bound water lifetimes. Compared to the other four chelates, the r_{2tot} for DyTETA is relatively independent of temperature due to the lack of water molecule exchange. Measurement errors for r_{2tot} and τ_M were less than 10% and 20%, respectively.

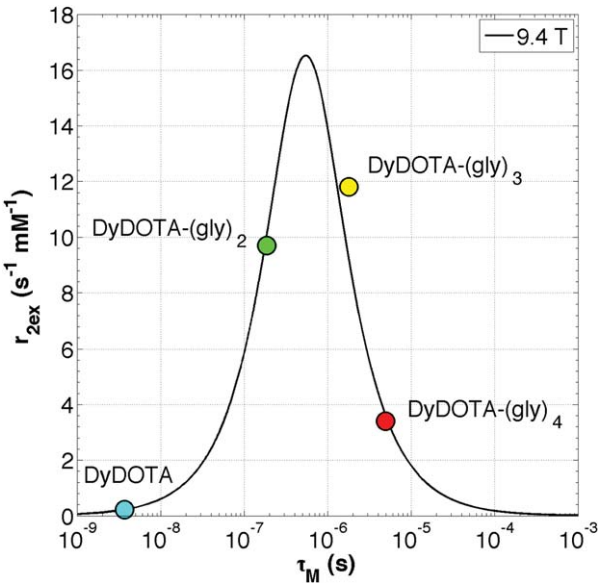

FIG. 4. A Swift-Connick plot for Dy^{3+} at 9.4T (400 MHz) using a $\Delta\omega$ of -730 ppm (1.835×10^6 rad s^{-1}). Data markers for the measured r_{2ex} and τ_M values at 37°C (from Table 1) are in excellent agreement with the Swift-Connick exchange theory, with DyDOTA-$(gly)_3$ giving the largest r_{2ex}.

reach a peak value of 16.5 s^{-1} mM^{-1} at a specific bound water lifetime given by $\Delta\omega^{-1} = 545$ ns. The "fast" side of the Swift-Connick plot is then defined as $\tau_M < 545$ ns, while the "slow" side is defined as $\tau_M > 545$ ns.

The 37°C data from Table 1 was plotted in Figure 4 for each DyDOTA-$(amide)_X$ chelate. It can be seen that the measured r_{2ex} and τ_M data are in excellent agreement with the Swift-Connick theory. For example, while the faster water molecule exchange rate of DyDOTA places it on the fast side of the Swift-Connick peak, the slower water molecule exchange rate of DyDOTA-$(gly)_4$ places it on the slow side. This explains why r_{2tot} decreases with increasing temperature (smaller τ_M) for DyDOTA, yet increases with increasing temperature for DyDOTA-$(gly)_4$. For DyDOTA-$(gly)_2$ and DyDOTA-$(gly)_3$, their intermediate water molecule exchange rates place them

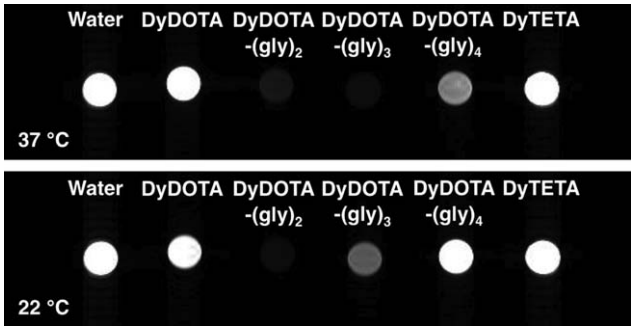

FIG. 5. Fast spin-echo images (TE = 12.4 ms) of the five Dy^{3+} chelates (and water standard) in 5 mm diameter vials taken at 9.4T. By taking the same image at two different temperatures the dependence of T_{2ex} (and thus the total T_2 contrast) upon the water molecule exchange rate can be qualitatively shown. The brightness and contrast levels for each image are the same.

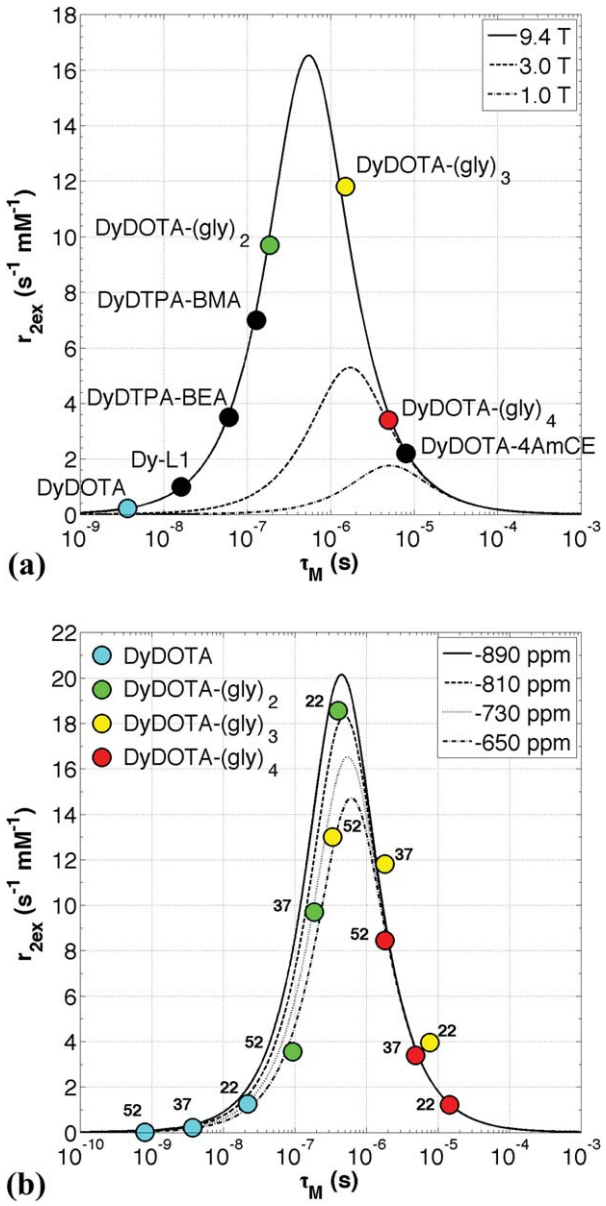

FIG. 6. **a**: A Swift-Connick plot comparing the new DyDOTA-$(amide)_X$ chelates (colored markers) to previous Dy^{3+}-based chelates (black markers) at 9.4T ($\Delta\omega = -730$ ppm or 1.835×10^6 rad s^{-1}) and 37°C. Also shown is a Swift-Connick plot for Dy^{3+} at 3.0T ($\Delta\omega = -730$ ppm or 5.871×10^5 rad s^{-1}). **b:** Swift-Connick plots for Dy^{3+} at 9.4T using four different values for $\Delta\omega$. Data markers for each chelate are shown (from Table 1) with temperatures given in °C. Note that the abscissa and ordinate ranges are different in (a) and (b).

close to the peak maximum in of the Swift-Connick plot. Figure 4 shows that at 37°C the highest r_{2ex} value is given by DyDOTA-$(gly)_3$ (11.8 s^{-1} mM^{-1} or 72% of the maximum r_{2ex}) making it a potential candidate for development into a T_2 contrast agent.

The effect that τ_M has on T_{2ex}, and thus the total T_2 contrast, can be qualitatively observed in the in vitro images shown in Figure 5. The top row shows a fast spin-echo image of a water standard and the five Dy^{3+} chelates (each at 20 mM) taken at 37°C. It can be seen that the signal intensities for DyDOTA (fast water molecule exchange) and DyTETA (no exchange) are similar to

that of pure water, indicating little or no T_2 contrast at this TE value (12.4 ms). Yet for the remaining three chelates, their level of T_2 contrast (i.e., darkening) is proportional to their vertical position (r_{2ex} value) on the Swift-Connick plot in Figure 4, with DyDOTA-$(gly)_3$ having the largest r_{2ex} value (11.8 s^{-1} mM^{-1}) and thus the darkest vial. The bottom row shows a similar fast spin-echo image but now at 22°C. The slower water molecule exchange at this temperature leads to different τ_M and thus r_{2ex} values for each DyDOTA-$(amide)_X$ chelate, with DyDOTA-$(gly)_2$ now having the largest r_{2ex} value (18.6 s^{-1} mM^{-1}) and the darkest vial (see Fig. 6b). Similar in vitro spin-echo images for two DyDTPA-based chelates at 4.7T and 25°C was shown by Vander Elst et al (19) where one vial appears darker simply due to the difference in τ_M and thus T_{2ex}.

DISCUSSION

It is interesting to compare these new DyDOTA-$(amide)_X$ chelates to previous Dy^{3+}-based T_2 contrast agents that have reported τ_M and r_2 data. Figure 6a displays experimental data (black symbols) for DyDOTA-4AmCE (35), DyDTPA-BMA (39), DyDTPA-BEA (19), and Dy-L1 (the Dy^{3+} analog of the Gd^{3+}-based human serum albumin binding MS-325 blood pool agent) (20,41) on a Swift-Connick plot for 9.4T ($\Delta\omega = -730$ ppm). The τ_M values at 37°C (calculated from ^{17}O data and Eq. [1] when not directly given) were 8 μs, 128.2 ns, 60 ns, and 16.1 ns, respectively. These τ_M values were then used to estimate the r_{2ex} values at 9.4T by means of Figure 6a, which gave 2.2, 7.0, 3.5, and 1.0 s^{-1} mM^{-1}, respectively. These estimated r_{2ex} values are in agreement with their previously reported r_2 data at 9.4T. It can be seen that these previous Dy^{3+} chelates all had water molecule exchange rates that were either too fast or too slow to maximize r_{2ex} at 9.4T. Although DyDTPA-BMA gives an r_{2ex} value of approximately 7 s^{-1} mM^{-1}, it is still less than half of the maximum (16.5 s^{-1} mM^{-1}). Due to their intermediate water molecule exchange rates at 37°C, both DyDOTA-$(gly)_2$ and DyDOTA-$(gly)_3$ give higher r_{2ex} values at 9.4T. Although the τ_M values for these two chelates are not quite at the ideal time of 545 ns, their r_{2ex} values are 59% and 72% the maximum respectively. These relative differences in r_{2ex} values become even more pronounced at fields lower than 9.4T, where the maximum r_{2ex} value reduces proportionately and moves toward slower exchange (larger τ_M) as shown in the 3.0T plot in Figure 6a. For example, at 9.4T (and 37°C) there is a 41% drop in r_{2ex} when moving from DyDOTA-$(gly)_3$ to DyDTPA-BMA (11.8 to 7.0 s^{-1} mM^{-1}), yet at 3.0T this reduction is 85% (5.3 to 0.8 s^{-1} mM^{-1}). Also, at 3.0T the peak r_{2ex} value of 5.3 s^{-1} mM^{-1} occurs at $\Delta\omega^{-1} = (5.871 \times 10^5 \text{ rad } s^{-1})^{-1} = 1703$ ns, which makes the DyDOTA-$(gly)_3$ chelate ($\tau_M = 1795$ ns at 37°C) ideally suited for use at 3.0T.

In Figure 4, it was assumed that all of the DyDOTA-$(amide)_X$ chelates studied here shared the same ^1H $\Delta\omega$ value of −730 ppm (11). Yet there is evidence from the r_{2ex} and τ_M data that the $\Delta\omega$ values do vary slightly between chelates. This should be expected because of their different chemical structures and ligand fields surrounding the Dy^{3+} ion. Figure 6b shows a Swift-Connick plot for Dy^{3+} at 9.4T (400 MHz) where four different values for $\Delta\omega$ have been plotted (see Eq. [2]). It can be seen that as the absolute value of $\Delta\omega$ increases, the maximum r_{2ex} value increases proportionally and moves toward faster exchange. It can also be seen that while there is little difference between the Swift-Connick plots on the slow side, where the four curves converge, there is a significant difference on the fast side and most notably in the peak maximum. By using the r_{2ex} data for all three temperatures measured in Table 1 and their corresponding calculated τ_M values, one can see how the r_{2ex} for each chelate varies with τ_M in Figure 6b. All of these data appear to be in fairly good agreement with $\Delta\omega = -730$ ppm except for DyDOTA-$(gly)_2$ at 22°C (green circle at $\tau_M = 400$ ns) which, due to its high r_{2ex} value of 18.6 s^{-1} mM^{-1}, appears to agree with a larger $\Delta\omega$ of around −810 ppm. Yet for DyDOTA-$(gly)_3$ at 52°C (yellow circle at $\tau_M = 330$ ns) the experimental r_{2ex} value of 13.0 s^{-1} mM^{-1} is more consistent with a lower $\Delta\omega$ of around −650 ppm, even though it shares a similar τ_M. This could be explained by the two chelates having different chemical fields that lead to different $\Delta\omega$ values and also by the variation of $\Delta\omega$ with temperature, where the absolute value of $\Delta\omega$ is inversely proportional to temperature. It is well known that hyperfine shifts such as these are extremely sensitive to temperature (42) so the exact shape and magnitude of these Swift-Connick type plots may depend upon getting a precise determination of $\Delta\omega$ from hyperfine shift measurements of other nonexchanging protons in these paramagnetic complexes by high resolution NMR spectroscopy. These observations agree with quantitative estimates of the bound water molecule ^1H $\Delta\omega$ made by measuring the chemical shifts of the cyclen H_4 protons in the DOTA ligand as a function of temperature (see Supplementary Material) (11).

CONCLUSIONS

These data represent the first time that T_{2ex} for a series of DyDOTA-$(amide)_X$ chelates has been optimized by methodically adjusting the inner-sphere water molecule exchange rate at 9.4T and 37°C. To achieve the goal of having an r_{2ex} value greater than 10 s^{-1} mM^{-1}, the τ_M needed to be in the "Goldilocks Zone" (43) (i.e., not too fast, not too slow, but just right) of approximately 200 ns to 2000 ns, with DyDOTA-$(gly)_3$ meeting this requirement ($\tau_M = 1800$ ns, $r_{2ex} = 11.8$ s^{-1} mM^{-1}) and DyDOTA-$(gly)_2$ coming close ($\tau_M = 190$ ns, $r_{2ex} = 9.7$ s^{-1} mM^{-1}). Preliminary in vivo results from the DyDOTA-$(gly)_2$ chelate showed a promising order of magnitude improvement in dose sensitivity compared with the EuDOTA-$(gly)_4$ chelate (44). Polymerization or dendrimerization of these chelates could further increase the r_{2ex} (per molecule) by a factor of 100 to approximately 1000 to 1200 s^{-1} mM^{-1} thereby creating highly sensitive, molecule-sized T_2 contrast agents for MRI. These data also stress the importance of selecting the correct water molecule exchange rate (and $\Delta\omega$) when designing lanthanide-based contrast agents as recently described by Sherry and Wu (45).

ACKNOWLEDGMENTS

The authors thank Dr. Yunkou Wu for his guidance with these experiments, and also acknowledge Dr. R.H.E.

Hudson and the University of Western Ontario ASPIRE award for supporting Mark Milne's visit to the Advanced Imaging Research Center at UT Southwestern.

REFERENCES

1. Lauterbur PC. Image formation by induced local interactions - examples employing nuclear magnetic-resonance. Nature 1973;242:190–191.
2. Damadian R, Goldsmith M, Minkoff L. NMR in cancer: XVI. FONAR image of live human body. Physiol Chem Phys M 1977;9:97–100.
3. Damadian R. Tumor detection by nuclear magnetic resonance. Science 1971;171:1151–1153.
4. Lauffer RB. Paramagnetic metal-complexes as water proton relaxation agents for NMR imaging - theory and design. Chem Rev 1987;87:901–927.
5. Caravan P, Ellison JJ, McMurry TJ, Lauffer RB. Gadolinium(III) chelates as MRI contrast agents: structure, dynamics, and applications. Chem Rev 1999;99:2293–2352.
6. Yoo B, Pagel MD. An overview of responsive MRI contrast agents for molecular imaging. Front Biosci 2008;13:1733–1752.
7. Viswanathan S, Kovacs Z, Green KN, Ratnakar SJ, Sherry AD. Alternatives to gadolinium-based metal chelates for magnetic resonance imaging. Chem Rev 2010;110:2960–3018.
8. Solomon I. Relaxation processes in a system of 2 spins. Phys Rev 1955;99:559–565.
9. Weissleder R, Elizondo G, Wittenberg J, Rabito CA, Bengele HH, Josephson L. Ultrasmall superparamagnetic iron-oxide - characterization of a new class of contrast agents for MR imaging. Radiology 1990;175:489–493.
10. Opina ACL, Ghaghada KB, Zhao PY, Kiefer G, Annapragada A, Sherry AD. TmDOTA-tetraglycinate encapsulated liposomes as pH-sensitive LipoCEST agents. Plos One 2011;6.e27370.
11. Zhang SR, Sherry AD. Physical characteristics of lanthanide complexes that act as magnetization transfer (MT) contrast agents. J Solid State Chem 2003;171:38–43.
12. Aime S, Barge A, Castelli DD, Fedeli F, Mortillaro A, Nielsen FU, Terreno E. Paramagnetic lanthanide(III) complexes as pH-sensitive chemical exchange saturation transfer (CEST) contrast agents for MRI applications. Magn Reson Med 2002;47:639–648.
13. Ward KM, Aletras AH, Balaban RS. A new class of contrast agents for MRI based on proton chemical exchange dependent saturation transfer (CEST). J Magn Reson 2000;143:79–87.
14. Vinogradov E, Sherry AD, Lenkinski RE. CEST: from basic principles to applications, challenges and opportunities. J Magn Reson 2013; 229:155–172.
15. Hancu I, Dixon WT, Woods M, Vinogradov E, Sherry AD, Lenkinski RE. CEST and PARACEST MR contrast agents. Acta Radiol 2010;51: 910–923.
16. Zhang S, Winter P, Wu K, Sherry AD. A novel europium(III)-based MRI contrast agent. J Am Chem Soc 2001;123:1517–1518.
17. Soesbe TC, Merritt ME, Green KN, Rojas-Quijano FA, Sherry AD. T(2) Exchange agents: a new class of paramagnetic MRI contrast agent that shortens water T(2) by chemical exchange rather than relaxation. Magn Reson Med 2011;66:1697–1703.
18. Pintacuda G, John M, Su XC, Otting G. NMR structure determination of protein-ligand complexes by lanthanide labeling. Acc Chem Res 2007;40:206–212.
19. Vander Elst L, Roch A, Gillis P, Laurent S, Botteman F, Bulte JWM, Muller RN. Dy-DTPA derivatives as relaxation agents for very high field MRI: the beneficial effect of slow water exchange on the transverse relaxivities. Magn Reson Med 2002;47:1121–1130.
20. Caravan P, Greenfield MT, Bulte JWM. Molecular factors that determine Curie spin relaxation in dysprosium complexes. Magn Reson Med 2001;46:917–922.
21. Swift TJ, Connick RE. NMR-relaxation mechanisms of O17 in aqueous solutions of paramagnetic cations and the lifetime of water molecules in the first coordination sphere. J Chem Phys 1962;37:307–321.
22. Rabenstein DL, Fan S. Proton nuclear-magnetic-resonance spectroscopy of aqueous-solutions – complete elimination of the water resonance by spin spin relaxation. Anal Chem 1986;58:3178–3184.
23. Aime S, Nano R, Grandi M. A new class of contrast agents for magnetic-resonance imaging based on selective reduction of water-T2 by chemical-exchange. Invest Radiol 1988;23:S267–S270.
24. Aime S, Calabi L, Biondi L, De Miranda M, Ghelli S, Paleari L, Rebaudengo C, Terreno E. Iopamidol: exploring the potential use of a well-established X-ray contrast agent for MRI. Magn Reson Med 2005; 53:830–834.
25. Aime S, Botta M, Barbero L, Uggeri F, Fedeli F. Water signal suppression by T2-relaxation enhancement promoted by Dy(Iii) complexes. Magn Reson Chem 1991;29:S85–S88.
26. Saeed M, Wendland MF, Tomei E, Rocklage SM, Quay SC, Moseley ME, Wolfe C, Higgins CB. Demarcation of myocardial ischemia - magnetic-susceptibility effect of contrast-medium in MR imaging. Radiology 1989;173:763–767.
27. Nilsson S, Wikstrom G, Ericsson A, Wikstrom M, Oksendal A, Waldenstrom A, Hemmingsson A. Myocardial cell death in reperfused and nonreperfused myocardial infarctions - MR imaging with dysprosium-DTPA-BMA in the pig. Acta Radiol 1996;37:18–26.
28. Nilsson S, Wikstrom G, Ericsson A, Wikstrom M, Oksendal A, Waldenstrom A, Hemmingsson A. Double-contrast mr imaging of reperfused porcine myocardial infarction - an experimental study using Gd-DTPA-BMA and Dy-DTPA-BMA. Acta Radiol 1996;37:27–35.
29. Saeed M, Wendland MF, Masui T, Higgins CB. Reperfused myocardial infarctions on T1- and susceptibility-enhanced MRI - evidence for loss of compartmentalization of contrast-media. Magn Reson Med 1994;31:31–39.
30. Zhao SH, Revel D, Arteaga C, Canet E, Liu SZ, Hadour G, Forrat R, Oksendal A. Magnetic susceptibility of Dy-DTPA-BMA to reperfused myocardial infarction in an excised dog heart model: evidence of viable myocardium. Chin Med J 2000;113:260–264.
31. Wang C, Sundin A, Ericsson A, BachGansmo T, Hemmingsson A, Ahlstrom H. Dysprosium-enhanced MR imaging for tumor tissue characterization - An experimental study in a human xenograft model. Acta Radiol 1997;38:281–286.
32. Roberts TPL, Kucharczyk J, Cox I, Moseley ME, Prayer L, Dillon W, Bleyl K, Harnish P. Sprodiamide-injection-enhanced magnetic resonance imaging of cerebral perfusion. Phase I clinical-trial results. Invest Radiol 1994;29:S24–S26.
33. Bulte JWM, Wu CC, Brechbiel MW, Brooks RA, Vymazal J, Holla M, Frank JA. Dysprosium-DOTA-PAMAM dendrimers as macromolecular T2 contrast agents - preparation and relaxometry. Invest Radiol 1998;33:841–845.
34. Fossheim SL, Kellar KE, Mansson S, Colet JM, Rongved P, Fahlvik AK, Klaveness J. Investigation of lanthanide-based starch particles as a model system for liver contrast agents. J Magn Reson Imaging 1999; 9:295–303.
35. Vander Elst L, Zhang S, Sherry AD, Laurent S, Botteman F, Muller RN. Dy-complexes as high field T2 contrast agents: influence of water exchange rates. Acad Radiol 2002;9:S297–S299.
36. Desreux JF. Nuclear magnetic-resonance spectroscopy of lanthanide complexes with a tetraacetic tetraaza macrocycle - unusual conformation properties. Inorg Chem 1980;19:1319–1324.
37. Kovacs Z, Sherry AD. A general-synthesis of 1,7-Disubstituted 1,4,7,10-tetraazacyclododecanes. J Chem Soc Chem Comm 1995:185–186.
38. Green KN, Viswanathan S, Rojas-Quijano FA, Kovacs Z, Sherry AD. Europium(III) DOTA-derivatives having ketone donor pendant arms display dramatically slower water exchange. Inorg Chem 2011;50: 1648–1655.
39. Pubanz D, Gonzalez G, Powell DH, Merbach AE. Unexpectedly large change of water exchange-rate and mechanism on [Ln(Dtpa-Bma)(H2o)] complexes along the Lanthanide(Iii) series. Inorg Chem 1995;34:4447–4453.
40. Granot J, Fiat D. Effect of chemical exchange on transverse relaxation rate of nuclei in solution containing paramagnetic-ions. J Magn Reson 1974;15:540–548.
41. Lauffer RB, Parmelee DJ, Dunham SU, Ouellet HS, Dolan RP, Witte S, McMurry TJ, Walovitch RC. MS-325: albumin-targeted contrast agent for MR angiography. Radiology 1998;207:529–538.
42. Peters JA, Huskens J, Raber DJ. Lanthanide induced shifts and relaxation rate enhancements. Prog Nucl Magn Reson Spectrosc 1996;28: 283–350.
43. Seager S. Exoplanet habitability. Science 2013;340:577–581.
44. Soesbe TC, Ratnakar JS, Kovacs Z, Sherry AD. Using T2-exchange from Dy3+DOTA-based chelates for contrast-enhanced molecular imaging with MRI. In Proceedings of the 21st Annual Meeting of ISMRM, Salt Lake City, Utah, USA, 2013. Abstract 1909.
45. Sherry AD, Wu YK. The importance of water exchange rates in the design of responsive agents for MRI. Curr Opin Chem Biol 2013;17: 167–174.

Advancing the early detection and diagnosis of primary and recurring thyroid cancers using a molecularly targeted T_2-exchange MRI contrast agent

Todd C. Soesbe[1,2*], S. James Ratnakar[1], Mark Milne[1], Fiemu Nwariaku[3], A. Dean Sherry[1,4], and Robert E. Lenkinski[2,1]

[1]Advanced Imaging Research Center, UT Southwestern Medical Center, Dallas, Texas. [2]Department of Radiology, UT Southwestern Medical Center, Dallas, Texas. [3]Department of Surgery, UT Southwestern Medical Center, Dallas, Texas. [4]Department of Chemistry, University of Texas, Dallas, Texas.

Target audience: This will benefit Scientists and Physicians interested in the chemical engineering, development, and pre-clinical *in vivo* imaging of molecularly targeted T_2 MRI contrast agents for the early detection and diagnosis of cancer. **Purpose**: The early detection and diagnosis of both primary and recurring cancerous lesions is essential to the successful treatment of aggressive thyroid cancer. Ultrasound imaging offers high-resolution and easy acquisition, but it lacks functional information, tissue specificity, and whole-body field of view capabilities. SPECT and PET offer very sensitive whole-body functional imaging, but suffer from low-resolution, warm and cold lesion indeterminacy, and require CT for anatomic correlation. Furthermore, dual-modality SPECT/CT and PET/CT expose the subject to significant doses of ionizing radiation, making them impractical for frequent therapeutic monitoring in patients. In contrast, MRI offers superior anatomic resolution and soft tissue contrast as compared to SPECT/CT and PET/CT, making it an excellent tool for cancer detection. The effectiveness of MRI in the functional and molecular imaging regime is currently limited due to the lack of highly sensitive molecularly targeted contrast agents. Creating such agents would greatly improve the use of MRI for the early detection and diagnosis of thyroid cancer. Our research goal is to use the newly described phenomena of T_2-exchange (T_{2ex}) to create highly sensitive, targeted, and molecule-sized T_2 contrast agents for enhanced molecular imaging of thyroid cancer with MRI. **Methods**: Four different versions of the DyDOTA-$(gly)_x$ chelate (i.e., x=0,2,3,4) were synthesized, with each chelate having a different water molecule exchange rate ($k_{ex}=\tau_M^{-1}$). The Dy^{3+} ion was used because it has the largest bound water chemical shift and one of the largest paramagnetic relaxation enhancements of the Lanthanide metals (second only to Gd^{3+}), both characteristics will maximize the level of T_2 contrast achieved for the monomer chelate ($r_2 \sim 16\ s^{-1}\ mM^{-1}$) as recently shown (1). The r_{2ex} and τ_M values for each chelate were then experimentally measured at 37 °C using ^{17}O methods (1). As proof of principle to show the negative contrast capabilities of these new T_{2ex} chelates, small doses were directly injected into mice brain and thyroid areas to simulate uptake due to molecular targeting. Animal data were acquired on an Agilent 9.4 T system.

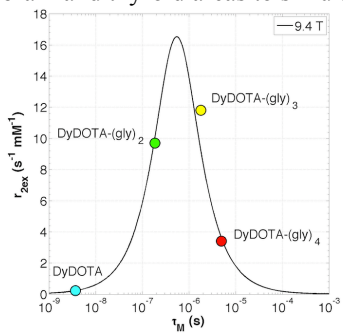

Fig. 1

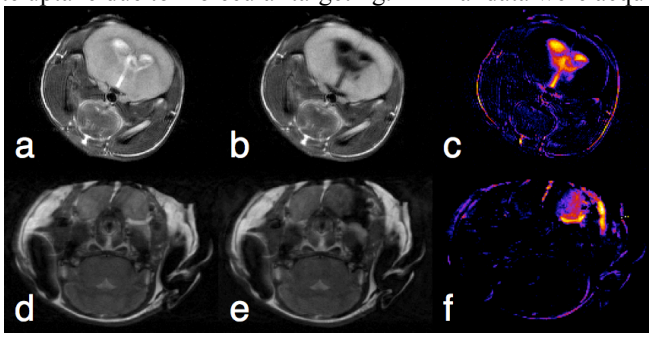

Fig. 2

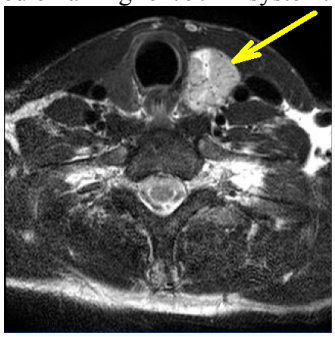

Fig. 3

Results: Fig. 1: A Swift-Connick plot showing the theoretical relation (black line) between the transverse relaxivity due to water molecule exchange (r_{2ex}; y-axis) and the bound water lifetime (τ_M; x-axis) for Dy^{3+} at 9.4 T. The ideal τ_M is at 545 ns. The measured r_{2ex} and τ_M values for the four different Dy^{3+} chelates (colored markers) are in excellent agreement, with DyDOTA-$(gly)_2$ (green circle) and DyDOTA-$(gly)_3$ (yellow circle) giving the highest r_{2ex} values. **Fig. 2**. **a**: Axial MRI of a healthy mouse brain before intracranial injection of 30 µmol/kg of DyDOTA-$(gly)_3$ in 20 µL **b**: After intracranial injection. Note the darkening of ventricle CSF due to T_{2ex}. **c**: The difference image a-b showing regions of agent uptake. **d**: Axial MRI of a healthy mouse thyroid before direct injection of 30 µmol/kg of DyDOTA-$(gly)_3$ in 20 µL **e**: After direct injection. Note the darkening of mouse's left thyroid/salivary gland area. **f**: The difference image d-e showing regions of agent uptake. **Fig. 3**: Axial MRI of a human thyroid nodule at 7.0 T. The nodule on patient's left (arrow), which appears bright under T_2 weighted MRI, would be an ideal target for a T_2 darkening contrast agent. Our goal is to target the cancerous regions of such nodules and lesions and make them "light up" as demonstrated in Fig. 2f. **Discussion**: We have previously shown that the Ln^{3+}DOTA-based chelates ($Ln^{3+}\neq$La, Gd, Lu) create enhanced T_2 contrast (i.e., darkening) in MRI through the chemical exchange of water molecules (2). The level of this "T_2-exchange" contrast is proportional to the bound water molecule chemical shift and reaches a maximum at a specific water molecule exchange rate. We have also previously demonstrated that T_{2ex} contrast can be increased by several orders of magnitude through simple linear polymerization of the Ln^{3+}DOTA chelate (3). We hypothesize that by using these two methods, a highly sensitive MRI T_2 contrast agent can be created while retaining the advantages of using small molecules rather than nanoparticles (e.g., SPIO) for improved biological targeting, uptake, and clearing. **Conclusion**: These T_{2ex} contrast agents have the potential to accurately image the location and size of cancerous thyroid lesions and (by using receptors as prognostic indicators) differentiate between indolent and aggressive forms, thereby performing disease staging entirely non-invasively (i.e., without FNA biopsy). Also, in contrast to SPECT/CT or PET/CT, disease diagnostics and therapy monitoring would be performed on a single-modality MRI instrument without the risk of ionizing radiation. This would reduce patient stress by eliminating unnecessary thyroid resections and finding recurrence earlier. This technique could also be combined with spectroscopy of the choline peak to increase specificity (4).

References: **(1)** Soesbe TC, et al. MRM 2014;71:1179-1185. **(2)** Soesbe TC, et al. MRM 2011;66:1697-1703. **(3)** Wu Y, Soesbe TC, et al., JACS 2008;130:13854-13855. **(4)** Mountford C, et al. JMRI 2006;24:459-477.